Available online at www.sciencedirect.com

SCIENCE DIRECT

Thin Solid Films 489 (2005) 296 – 302

www.elsevier.com/locate/tsf

Enhanced phosphorescence and electroluminescence in triplet emitters by doping gold into cadmium selenide/zinc sulfide nanoparticles

Hong-Wei Liu, Inamur R. Laskar, Chin-Ping Huang, Jung-An Cheng, Shih-Shun Cheng, Li-Yang Luo, Huei-Ru Wang, Teng-Ming Chen*

Department of Applied Chemistry, National Chiao Tung University and UST-CNST, Hsinchu 30050, Taiwan

Received 16 September 2004; received in revised form 7 February 2005; accepted 27 April 2005
Available online 15 June 2005

Abstract

Gold–cadmium selenide/zinc sulfide (Au–CdSe/ZnS) nanocomposites (NCs) were synthesized and characterized by transmission electron microscopy (TEM), energy dispersive X-ray (EDX) analysis, ultraviolet–visible (UV–visible) absorption and photoluminescence (PL) emission spectroscopy. The PL intensity in the Au–CdSe/ZnS NCs system was found to be much greater than that of CdSe/ZnS nanoparticles (NPs) alone, because of the surface-enhanced Raman scattering of Au NPs. Adding Au–CdSe/ZnS NCs to the cyclometalated iridium(III) complex (Ir-complex) greatly enhanced the PL intensity of a triplet emitter. Three double-layered electroluminescence (EL) devices were fabricated where the emitting zone contains the definite mixture of Ir-complex and the NCs [molar concentration of Ir-complex/NCs = 1:0 (Blank, D-**1**), 1:1 (D-**2**) and 1:3 (D-**3**)] and the device D-**2** exhibited optimal EL performances.

PACS: 71.55.Gs; 73.21.La
Keywords: II–VI semiconductors; Doping; Quantum dots; Electroluminescence

1. Introduction

CdSe quantum dots (QDs) exhibit size-dependent tunable photoluminescence (PL) with broad excitation spectra and narrow emission bandwidths that span the visible spectrum. Therefore, they are potentially useful in a wide range of applications [1–3]. These characteristics of semiconductor CdSe QDs have inspired scientific communities to fabricate hybrid organic light emitting diodes (OLEDs), which combine the diversity of organic materials with the excellent electronic and optical properties of inorganic materials. Coe et al. reported [4] the fabrication of a hybrid OLED, where QDs function exclusively as lumophores. Recently, Chaudhary et al. [5] demonstrated a trilayer polymer-quantum dot OLED which was fabricated by sandwiching a CdSe/ZnS QDs layer between films of polyvinylcarbazole (PVK) and butyl-oxadiazole derivative. The benefit of such a QD-based OLED is that each recombination of a hole and an electron generates a photon, resulting in a possible 100% quantum efficiency at any visible wavelength, since the tuning property of the emission wavelengths depends on the variability of the QDs' size. In most hybrid OLED devices, the ODs themselves act as light emitting centers [4–6]. For the first time, we reported elsewhere [7] that the enhancement of quantum efficiency of a triplet iridium(III) complex (Ir-complex) emitter in the presence of CdSe/ZnS QDs in the emitting layer of OLED.

The nonlinear response of composites of nanoparticles (NPs) with a metal and semiconductor suspended in a nonlinear medium exhibited was several orders of magnitude stronger than that of each of their components [8–11]. A strong surface-enhanced Raman scattering (SERS) effect was observed in Au/semiconductor or Ag/semiconductor colloidal nanocomposites (NCs) [8–12]. Nayak et al.

* Corresponding author. Tel.: +886 35731695; fax: +886 35723764.
E-mail addresses: howeliu.ac89g@nctu.edu.tw (H.-W. Liu), tmchen@mail.nctu.edu.tw (T.-M. Chen).

0040-6090/$ - see front matter © 2005 Elsevier B.V. All rights reserved.
doi:10.1016/j.tsf.2005.04.094

generated Au–CdSe NCs [13], although a large fraction of the particles was a mixture of individual gold and CdSe NPs, as indicated by transmission electron microscopy (TEM) micrographs. Enhanced optoelelectronic properties have been extensively reported and have been determined from the SERS activity of Au and Ag metallic NPs [14,15]. These facts motivated the exploration herein of the optical and electronic properties of metallic NPs and CdSe NPs and observations of the effect of these NPs on the PL and electroluminescence (EL) of a triplet emitter. This work reports the syntheses and characterizations of Au–CdSe/ZnS NCs and their applications in enhancing the thin-film PL and EL efficiencies of a triplet iridium(III) emitter when the NCs incorporated into the triplet emitter in the emitting layer of a hybrid OLEDs.

2. Experimental details

2.1. Chemicals and reagents

Hydrogen tetrachloroaurate (III) and tetraoctylammonium bromide were purchased from Acros Chemicals Company. Cadmium oxide (~1 μm, 99.5%), selenium (Se) powder (~100 mesh, 99.5+%), zinc acetate dehydrate (>98%), polyvinylcarbazole (PVK) and sulfur powder (99.8%) were all purchased from Aldrich Chemicals, USA. 1-Hexadecylamine (HDA, 98+%), lithium fluoride (LiF) and aluminum (Al) were obtained from Lancaster. Tri-*n*-butylphosphine (TBP) was obtained from Showa Chemicals Company, Japan. Anhydrous toluene and chloroform were purchased from TEDIA. Bis(4-trifluoro-methyl)-2-phenyl-benzothiazolatoacetylacetonate-iridium(III) (Ir-complex) was synthesized following the method reported in the literature [16].

2.2. Preparation of Au NPs

The Au NPs were synthesized according to the method reported in the literature [17]. A 25 ml aqueous solution of $HAuCl_4$ (0.3 mmol) was added to an 80 ml toluene solution of tetraoctylammonium bromide (1.8 mmol). The transfer of the Au metal salt to the toluene phase was clearly visualized within a few seconds. 25 ml of 0.25 M $NaBH_4$ solution was then added to the stirred mixture, resulting immediately to reduction. The toluene phase was then saved and the water phase was removed.

2.3. Preparation of Au–CdSe/ZnS NCs

A mixture of Au and CdSe/ZnS NPs with 0.02:1 in molar ratio was prepared as follows. CdO (0.6 mmol) and HDA (9 mmol) were dissolved in 20 ml of tributlyphosphine (TBP). The reaction mixture was then heated at 260 °C for 2 h under nitrogen atmosphere. 4 ml of Au NPs (3×10^{-3} M) was injected into the reaction mixture. The prepared Se solution (0.7 mmol of Se in 5 ml TBP solution) was immediately injected into the reaction mixture, which was kept at the desired temperature (160–260 °C) for 1 min. Then, zinc acetate (0.1 mmol) and sulfur (0.12 mmol) were dissolved in 5 ml of TBP, and injected into the reaction mixture. The temperature of the reaction mixture was maintained at 120 °C for 0.5 h. Toluene was injected into the reaction vessel. Other nanocomposites of Au and CdSe/ZnS NPs with different stoichiometries have been prepared following the method described above and all of the samples were dispersed and stored in toluene.

2.4. Instrumentations

Raman scattering spectra were obtained using a Jobin Yvon HR 800 spectrometer and a He–Ne laser as a light source. A Jeol JEM-4000EX TEM operated at 200 kV was used to determine the microstructure of QDs and their composition was analyzed using energy dispersive X-ray (EDX) analysis. PL excitation and ambient temperature emission spectra were measured using a Jobin Yvon Spex Fluorolog 3 spectrofluorometer with a monochromatized Xe light source (300 W). The emission spectra of various NCs were obtained at an excitation wavelength (λ_{ex}) of 367 nm. Ultraviolet–visible (UV–visible) absorption spectra of NCs were measured using a Hitachi U-3010 UV–visible spectrophotometer. The concentration of the samples for PL and UV–visible measurements was maintained at the concentration of 1×10^{-4} M in toluene. The fluorescence decay lifetimes were obtained by time-correlated single photon counting (TCSPC; Fluo Time 200, Pico-Quant) and the samples were excited by using a short pulse diode laser (LDH-P-C 375, Pico-Quant) at 375 nm.

2.5. Fabrication of thin films and EL devices

By spinning from concentrated dispersions in chloroform (3 ml) on flat quartz substrate (i.e., Ir-complex:Au–CdSe/ZnS=1:0 to 1:5), we have fabricated several uniform thin films comprising a fixed number of moles of Ir-complex with various molar concentrations of Au–CdSe/ZnS NCs in a fixed amount of Au–CdSe/ZnS PVK matrix. The 1:1 mixture of Ir-complex and Au–CdSe/ZnS NCs (Au:CdSe/ZnS=0.001:1) were prepared as follows. 1 ml of Ir-complex (1.6×10^{-6} M) was mixed with 0.016 ml of Au–CdSe/ZnS (1×10^{-4} M) in chloroform. Similarly, we have prepared other Ir-complex and Au–CdSe/ZnS NCs mixture solutions proportionately. Then, 30 mg of PVK was added to each of the mixtures and the total volume was kept constant to 3 ml by adding chloroform. The thicknesses of the thin films were measured by the alpha-stepper method at various arbitrary points (8±0.5 nm).

A series of double-layered EL device with structure represented in Fig. 1 were designed and fabricated. These devices mainly contain green-emitting Au–CdSe/ZnS NCs doped with the orange-emitting iridium(III) triplet emitter in

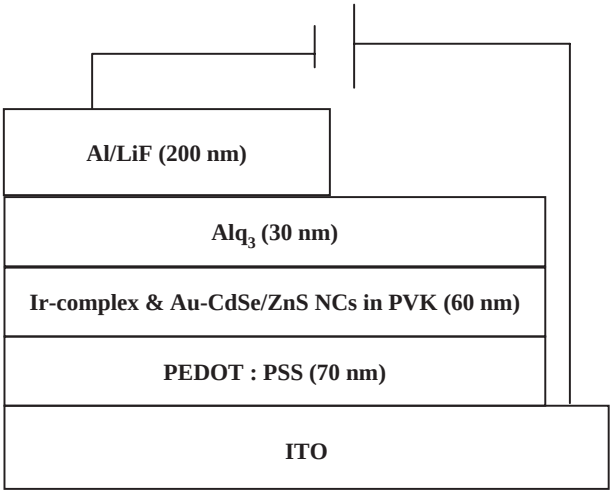

Fig. 1. The EL device structure with Au–CdSe/ZnS NCs and Ir-complex in PVK matrix as emitting material.

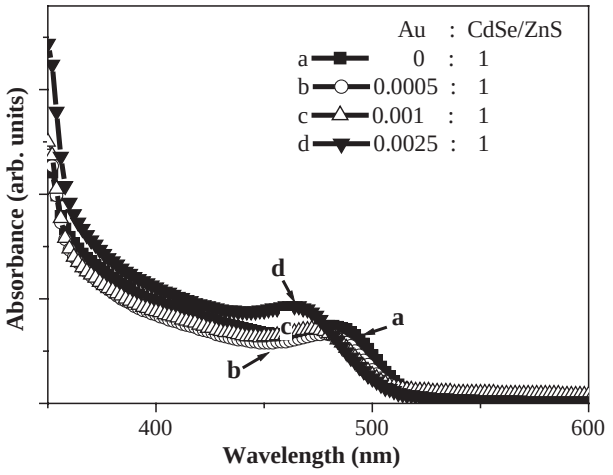

Fig. 2. UV–visible absorption spectra of CdSe/ZnS NPs and Au–CdSe/ZnS NCs in toluene (concentration = 1×10^{-4} mol/L); Au–CdSe/ZnS NCs show blue-shifted absorbance as compared to CdSe/ZnS NPs.

different proportions in the emitting layer. The emitting layer contains Ir-complex and Au–CdSe/ZnS NCs in PVK matrix with the molar ratios of 1:0 (Blank, D-**1**), 1:1 (D-**2**) and 1:3 (D-**3**), respectively. The emitting components were spin-cast from chloroform onto the poly(3,4-ethylenedioxythiophene) (PEDOT)/poly(4-styrenesulfonate) (PSS)-coated indium tin oxides (ITO) glass substrates. Tris(8-hydroxyquinolinato)aluminum(III) (Alq_3) was subsequently spin-cast onto the emitting layers and LiF/Al cathode was vacuum-deposited on top of the emitting layers at 1.3×10^{-4} Pa. The layer sequences and the thicknesses of each layer were the same across the three fabricated devices. The current–voltage profiles and EL intensity characteristics of the above fabricated devices were measured in a vacuum chamber at 1.3×10^{-4} Pa at ambient temperature using a Keithley 2400 source meter-2000 multimeter, coupled to a PR 650 optical meter.

3. Results and discussions

Au–CdSe/ZnS NCs, stabilized in toluene, were successfully synthesized. Fig. 2 presents the UV–visible spectra of the CdSe/ZnS NPs and Au–CdSe/ZnS NCs. The sample of CdSe/ZnS NPs alone was found to absorb at 490 nm. At an Au NPs concentration of 0.0025 mol per mol of CdSe/ZnS NPs, the absorption wavelength was found to be blue-shifted with respect to CdSe/ZnS NPs by approximately 20 nm. In general, the Au colloids exhibit absorption with a maximum at 530 nm identified as a surface plasmon band, which was similar to that suggested by Gittins and Caruso [17]. However, as presented by Fig. 2, no surface plasmon band was observed, indicating that the concentration of Au NPs is not sufficiently high to reveal the band. The Au NPs are probably covered by CdSe/ZnS NPs, such as Au/CdS NCs [18]. Surfactants tend to make Au–CdSe/ZnS NCs less responsive to UV–visible. However, possible electron transfer from CdSe/ZnS NPs to Au was assumed to be responsible for the bleaching of the surface plasmon band and to occur within few picoseconds [18]. Therefore, the absorption actually was observed from the CdSe/ZnS NPs.

Fig. 3 displays a series of solution PL spectra for samples of Au–CdSe/ZnS NCs with various molar ratios of Au to CdSe/ZnS in toluene. The emission of Au–CdSe/ZnS was slightly blue-shifted from that of pure CdSe/ZnS NPs. Surprisingly, the PL intensity of Au–CdSe/ZnS NCs was found to exceed that of CdSe/ZnS NPs. The highest PL intensity was found for the sample with the molar ratio Au:CdSe/ZnS = 0.001:1 and the PL intensity was found to be 1.5 times higher than that of CdSe/ZnS. The observed dramatic increase in the PL intensity of Au–CdSe/ZnS NCs was probably attributable to the SERS activity of Au metal in Au–CdSe/ZnS NCs [14,19]. When more Au NPs were incorporated into CdSe/ZnS NPs, the concentration

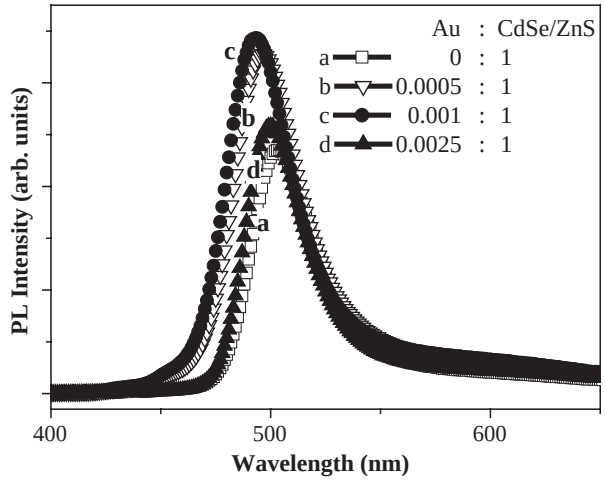

Fig. 3. Comparative PL intensity of CdSe/ZnS NPs and Au–CdSe/ZnS NCs in toluene (concentration = 1×10^{-4} mol/L).

quenching of PL intensity of Au–CdSe/ZnS NCs is expected.

The diameter of Au NPs was around 5 nm and that of green-emitting CdSe/ZnS NPs was ~1 nm as determined by TEM [deposited]. Fig. 4(a) shows the TEM image of Au–CdSe/ZnS NCs where the amount of CdSe/ZnS NPs used to prepare Au–CdSe/ZnS NCs was 50 times larger than that of the Au-precursor. This large quantity of CdSe/ZnS NPs used with respect to the Au NPs suggests that almost all the Au particles have been covered by the CdSe/ZnS NPs. It has been supported by the observed diameters of the particles shown in the TEM image (Fig. 4(a)) which falls in the range of 6–8 nm. A similar observation has also been reported earlier by Kamat and Shanghavi [18] in their study of Au/CdS composite nanoclusters. The characteristic EDX elemental analytical data represented in Fig. 4(b) demonstrate the presence of Au, Cd, Se, Zn and S, supporting the formation of Au–CdSe/ZnS NCs.

Fig. 5 represents the Raman spectra of Au NPs, CdSe/ZnS NPs and Au–CdSe/ZnS NCs (with Au: CdSe/ZnS = 1/50). It was suggested that the SERS activity of the gold NPs was supported by the observed strong enhancement in the

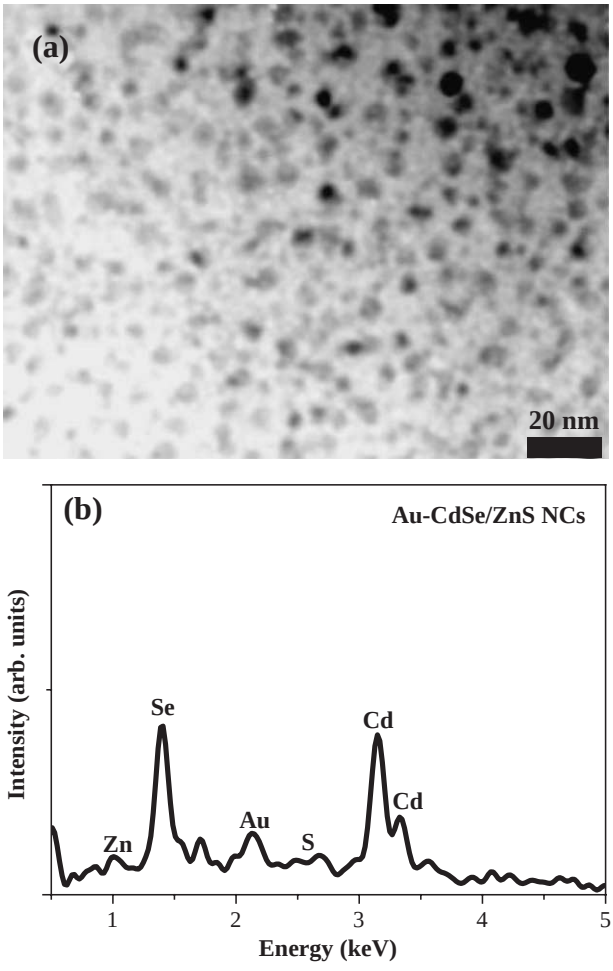

Fig. 4. (a) TEM micrograph of Au–CdSe/ZnS NCs and (b) EDX elemental analysis for Au–CdSe/ZnS NCs.

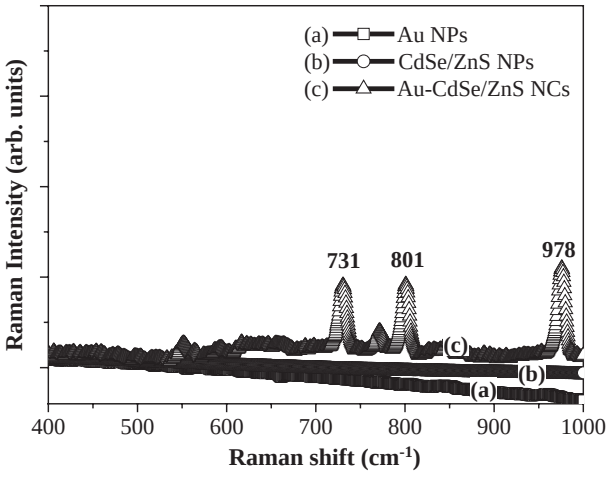

Fig. 5. Raman scattering spectra for the (a) Au NPs, (b) CdSe/ZnS NPs and (c) Au–CdSe/ZnS NCs (Au:CdSe/ZnS = 1:50). Raman signals are clearly observed in Au–CdSe/ZnS hybrid NPs.

Raman signal [20,21] in Au–CdSe/ZnS NCs. In the given spectral range, several Raman peaks at 731 cm^{-1}, 801 cm^{-1} and 978 cm^{-1} were observed in the sample of Au–CdSe/ZnS with a high proportion of Au in CdSe/ZnS (with Au:CdSe/ZnS = 1/50) (as shown in Fig. 5), whereas no discernible Raman features were observed from the bare Au and CdSe/ZnS NPs. It is proposed that the increased PL intensity (as shown in Fig. 3) is attributed to the presence of the SERS-active Au NPs.

The Strickler–Berg relation [22] was used to determine the radiative lifetime (τ_R) of CdSe/ZnS and Au–CdSe/ZnS NCs. The fluorescence decay was examined by TCSPC techniques and the average lifetime (τ_S) was obtained [22]. The number of photon emission per electron absorption (quantum yield) of Au–CdSe/ZnS NCs was calculated from Eq. (1).

$$\text{Quantum yield} = \frac{\tau_S}{\tau_R} \quad (1)$$

As depicted in Table 1, optimal fluorescence quantum yield was obtained for the NCs with Au:CdSe/ZnS = 0.001:1 and at the same concentration the maximum quantum yield was found to be almost 1.5 times higher than that of CdSe/ZnS NPs (without Au doping).

Table 1
Room-temperature luminescence and decay parameters for Au–CdSe/ZnS NCs samples with various ratios of CdSe/ZnS and Au NPs in toluene

Au:CdSe/ZnS (molar ratio)	PL (λ_{max})	τ_R[a] (ns)	τ_S[b] (ns)	Quantum yield[c]
0:1	507	31.8	14.1	0.44
0.0005:1	502	31.9	20.7	0.65
0.001:1	498	29.8	20.7	0.69
0.0025:1	501	27.2	16.5	0.61

[a] Radiative lifetime was calculated by using Strickler–Berg relation.
[b] Average decay time at room temperature.
[c] Quantum yield = τ_S/τ_R.

Many optical and physical properties of colloidal CdSe NPs, including their energy transfer mechanism and excited-state lifetime, are not yet well understood. The Ir-complex is a good phosphorescent material for use in OLEDs and CdSe NPs is a fluorescence material with excellent optical characteristics. It is interesting to observe the effect on PL intensity/quantum efficiency of an Ir-based triplet emitter on gradual increasing of molar concentration of Au–CdSe/ZnS NCs into the Ir-complex. A series of thin films were fabricated, in which the amount of Au–CdSe/ZnS NCs was varied by increasing the molar proportions of Au–CdSe/ZnS NCs, while the molar concentration of Ir-complex was held constant (see Section 2). Fig. 6(a) indicates that the PL intensity dramatically increased with the doping concentrations of Au–CdSe/ZnS NCs at an exciting wavelength, 330 nm. Fig. 6(a) reveals that the PL emission intensity was maximum for the composition Ir-complex:Au–CdSe/ZnS=1:3 and was approximately 10 times greater than that of the blank Ir-complex.

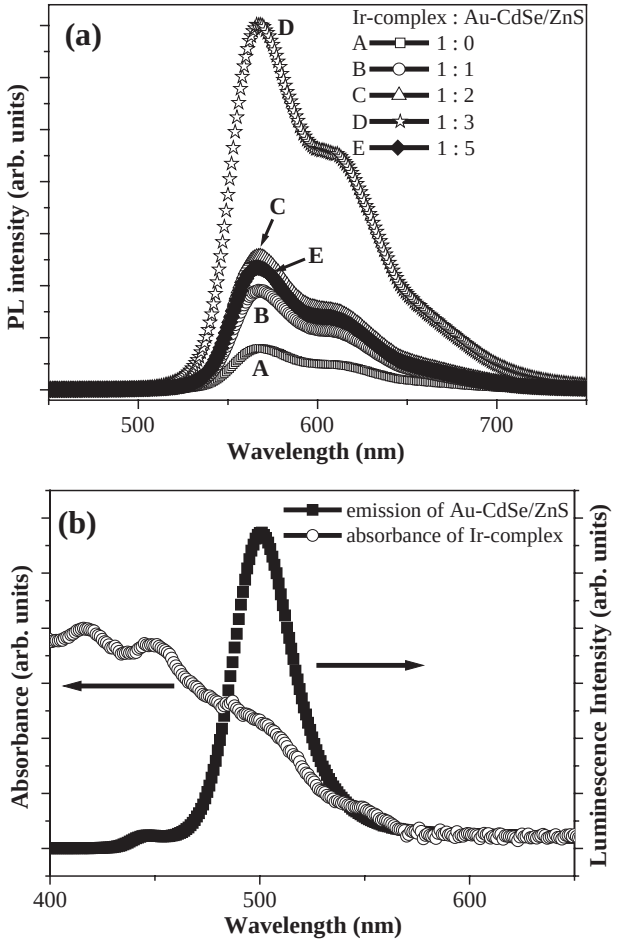

Fig. 6. (a) Solid-state thin-film PL spectra of fixed molar concentration of Ir-complex incorporated by Au–CdSe/ZnS NCs in PVK matrix with different molar concentration. (b) UV–visible absorption spectrum of Ir-complex in PVK matrix and PL spectrum of Au–CdSe/ZnS NCs in the PVK matrix, showing the overlapping region.

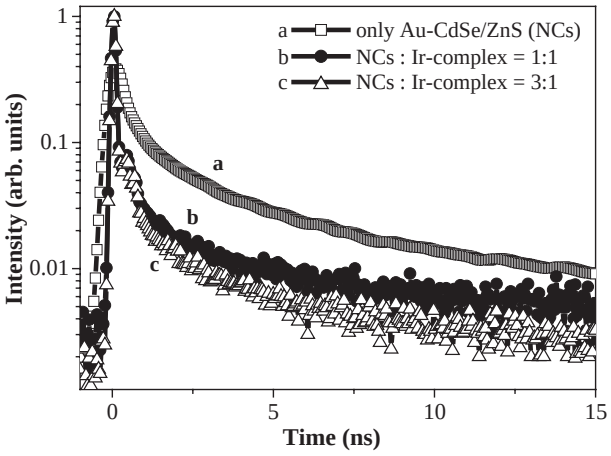

Fig. 7. Time-resolved photoluminescence of decay curves of the Au–CdSe/ZnS NCs films doped with the Ir-complex.

Fig. 6(b) presents the UV–visible absorption spectra of the Ir-complex doped in the thin film with PVK as a matrix. Several broad absorption bands of metal to ligand charge transfer transitions (^{1}MLCT and ^{3}MLCT) [16] from 375 nm to 575 nm, and the emission spectrum of CdSe NPs excited by light with a wavelength of 330 nm were observed. The emissive region (360–600 nm) of Au–CdSe/ZnS NCs was clearly found to overlap with the absorptive part of the Ir-complex, suggesting that the photons were effectively absorbed by both NCs and the Ir-complex, and that the energy absorbed by the NCs was transferred efficiently to the Ir-complex triplet emitter, increasing the PL intensity, as observed [23]. The Ir-complex was a phosphorescent material with strong emission around 575 nm. The aggregation of NCs in the solid film was such that the PL emission of NCs was too weak to be observed clearly in Fig. 6(a).

It has been attempted to explore the energy transfer mechanism involved in the Ir-complex/NCs thin films. In this case, the fluorescence decay of NCs was determined based on time-resolved luminescence measurements, as shown in Fig. 7. It is observed that the fluorescence decay lifetime for mixtures of Au–CdSe/ZnS NCs and Ir-complex is much shorter than that of bare NCs. When each of the decay kinetics was treated as a two-exponent curve [24,25], it was deconvoluted and resolved as slow and fast components of decay. Due to the pulse limitation of TCSPC, it was only possible to resolve the component of slow decay. As shown in Fig. 7, the PL lifetime for the mixtures containing Au–CdSe/ZnS NCs and Ir-complex is much shorter than that of Ir-free NCs alone, which also supports the energy transfer from NCs to the triplet emitter [26]. Hence, it can be proposed that the enhanced luminescence of Ir-complex can probably be attributed to non-radiative energy transfer from the NCs to Ir-complex. The decay lifetime decreases from 4.0 ns (for sample of Au–CdSe/ZnS NCs alone) to 2.6 ns (for sample with Ir-complex:NCs=1:1) and 2.0 ns (for that with Ir-complex:NCs=1:3), respectively.

If the observed slow decay of the donor (NCs) following pulse excitation is a single exponential, then the measurement of the decay lifetime in the presence (τ_D) and absence (τ_0) of energy transfer is a straightforward method of determining the transfer rate constant, in that case the efficiency of the energy transfer can be determined by using time-resolved method [22]. The efficiency of energy transfer can be described by Eq. (2):

$$\text{Efficiency of energy transfer} = \frac{\tau_0 - \tau_D}{\tau_0}. \quad (2)$$

The efficiency of energy transfer calculated from the above equation was found to be 35% and 51% for the samples of Ir-complex and Au–CdSe/ZnS NCs having molar ratios of 1:1 and 1:3, respectively.

The EL devices were designed and fabricated with the structure depicted in Fig. 1. EL luminance was found to be maximal in the device D-**2**, but that for D-**3** was found to be lower than that of D-**1**, as presented in Fig. 8. Luminescence decay in D-**3** was attributed to quenching in the device with a higher concentration of Au–CdSe/ZnS NCs. As revealed by the PL spectra represented in Fig. 6(a), the main EL emission of the three devices originated from the Ir-complex, while the electron transport material Alq_3 was associated with the weaker emission around 520 nm. Table 2 presents the comparative EL characteristics of all fabricated devices. At a fixed current density (44.5 mA/cm^2), D-**2** performed best among the three devices and the corresponding EL luminance was found to be 521 cd/m^2. All three devices exhibited similar commission internationale del'Eclairage 1931 (CIE 1931) coordinates and maximal emission wavelength. Excitons are suggested to be generated in the Ir-complex via two parallel processes. Firstly, excitons are generated on NCs and then Förster-type energy transfer undergoes efficiently to the Ir-complex, and secondly, direct charge trapping by the Ir-complex occurs. The excitons on the Ir-complex subsequently decay radiatively.

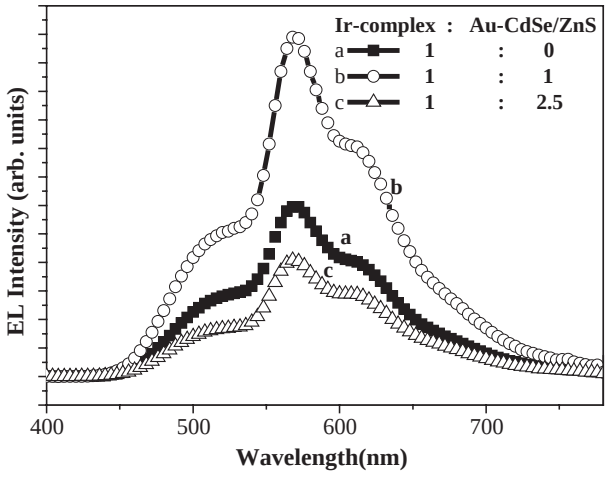

Fig. 8. EL emission spectra of the fabricated devices with different molar proportions of the Ir-complex and Au–CdSe/ZnS NCs as emitting layer in PVK matrix.

Table 2
Comparative EL characteristics of all fabricated devices (D-**1**, D-**2** and D-**3**) at a fixed current density of 44.5 mA/cm^2

EL characteristics	D-**1**	D-**2**	D-**3**
External quantum yield (cd/A)	0.8	1.2	0.7
Luminance (cd/m^2)	353	521	267
Drive voltage (V)	5.5	5.9	7.2
CIE 1931 value (x, y)	(0.45, 0.49)	(0.46, 0.49)	(0.46, 0.49)
λ_{max} of EL (nm)	568	568	568

The quantum efficiency of the present device was not found as we expected for the previous devices fabricated based on only CdSe/ZnS NPs [7]. As presented in Fig. 8, the broad emission of the three devices observed near 520 nm was associated primarily with the electron transport material Alq_3. This observation suggests that the recombination of holes and electrons in the emitting zone was ineffective, leading to low quantum efficiency. A hole-blocking layer between the emitting and electron transport layers can be assumed to be required to confine the holes and electrons in the emitting zone. More attempts will be made to improve the efficiency of this device in the future.

4. Conclusion

A series of Au–CdSe/ZnS NCs with significantly higher quantum efficiencies than only CdSe/ZnS NPs were synthesized and characterized. The observed enhancement of PL and EL intensity and the quantum efficiencies of fabricated EL devices supported the observed efficient energy transfer from the Au–CdSe/ZnS NCs to the triplet iridium(III) emitter. The energy transfer has also been evidenced by the time-resolved PL measurement. The enhancement in the PL intensity of the Ir-complex observed in the thin-film sample was found to increase with the doping concentration of Au–CdSe/ZnS NCs in the emissive layer, but the EL performance was not as expected. This investigation demonstrated that the novel energy transfer from the NCs to the Ir-complex is of great interest and reveals the feasibility of applying NCs in hybrid OLEDs. The authors are now focusing on improving device performance by either optimizing the thicknesses of the layers or incorporating a hole-blocking layer between the emitting and electron transport layers.

Acknowledgements

This research is partly supported by National Science Council of Taiwan, ROC under the contract nos. NSC91-2816-M-009-0002-6 and NSC 93-2120-M-009-008. We also acknowledge funding support from Center for Nano-Science and Technology, University System of Taiwan (UST-CNST) in FY 2004. Professors K.H. Wei, C.S. Hsu and Eric W.G. Diau are acknowledged for helpful discussions.

Appendix A. Supplementay data

Supplementary data associated with this article can be found, in the online version, at doi:10.1016/j.tsf.2005.04.094.

References

[1] M. Bruchez, M. Moronne, P. Gin, S. Weiss, A.P. Alivisatos, Science 281 (1998) 2013.
[2] W.C.W. Chan, S.M. Nie, Science 281 (1998) 2016.
[3] H. Mattoussi, L. Radzilowski, B. Dabbousi, E. Thomas, M. Bawendi, M. Rubner, J. Appl. Phys. 83 (1998) 7965.
[4] S. Coe, W.-K. Woo, M. Bawendi, V. Bulovic, Nature 420 (2002) 800.
[5] S. Chaudhary, M. Ozkan, W.C.W. Chan, Appl. Phys. Lett. 84 (2004) 2925.
[6] T. Tsutsui, Nature 420 (2002) 752.
[7] I.R. Laskar, H.W. Liu, C.P. Huang, J.A. Cheng, T.M. Chen, Jpn. J. Appl. Phys. Lett. 44 (2005) L727.
[8] I. Honma, T. Sano, H. Komiyama, J. Phys. Chem. 97 (1993) 6692.
[9] M. Kerker, C.G. Blatchford, Phys. Rev., B 26 (1982) 4052.
[10] T.M. Cotton, R.A. Uphaus, D. Mobius, J. Phys. Chem. 90 (1986) 6071.
[11] M. Kerker, O. Siiman, D.S. Wang, J. Phys. Chem. 88 (1984) 3168.
[12] G. Oldfield, T. Ung, P. Mulvaney, Adv. Mater. 12 (2000) 1519.
[13] R. Nayak, J. Galsworthy, P. Dobson, J. Hutchinson, J. Mater. Res. 13 (1998) 905.
[14] J.H. Park, Y.T. Lim, O.O. Park, Y.C. Kim, Macromol. Rapid Commun. 24 (2003) 331.
[15] J.W. Hu, G.B. Han, B. Ren, S.G. Sun, Z.Q. Tian, Langmuir 20 (2004) 8831.
[16] I.R. Laskar, T.-M. Chen, Chem. Mater. 16 (2004) 111.
[17] D.I. Gittins, F. Caruso, Angew. Chem., Int. Ed. 40 (2001) 3001.
[18] P.V. Kamat, B. Shanghavi, J. Phys. Chem., B 101 (1997) 7675.
[19] J.H. Park, Y.T. Lim, O.O. Park, J.K. Kim, J.-W. Yu, Y.C. Kim, Chem. Mater. 16 (2004) 688.
[20] T. Zhu, X. Zhang, J. Wang, X. Fu, Z. Liu, Thin Solid Films 327–329 (1998) 595.
[21] S. Sanchez-Cortes, C. Domingo, J.V. Garcia-Ramos, J.A. Aznarez, Langmuir 17 (2001) 1157.
[22] B. Valeur, Molecular Fluorescence: Principles and Applications; Wiley-VCH: New York; 2002 p. 42, 172.
[23] A.R. Clapp, I.L. Medintz, J.M. Mauro, B.R. Fisher, M.G. Bawendi, H. Mattoussi, J. Am. Chem. Soc. 126 (2004) 301.
[24] X.Y. Wang, J.Y. Zhang, A. Nazzal, M. Darragh, M. Xiao, Appl. Phys. Lett. 81 (2002) 4829.
[25] B.R. Fisher, H.J. Eisler, N.E. Stott, M.G. Bawendi, J. Phys. Chem., B 108 (2004) 143.
[26] Z. Tang, B. Ozturk, Y. Wang, N.A. Kotov, J. Phys. Chem., B 108 (2004) 6927.